

CHARACTERISTICS OF WAVEPACKET AND WEDGE-SHAPED DISTURBANCES PROPAGATING IN A SUPERSONIC BOUNDARY LAYER

Takashi Atobe*, Hsun H. Chen**

*Japan Arospace Exploration Agency, **California State University, Long Beach

Keywords: *Supersonic flow. boundary layer. transition. saddle point method. complex ray theory*

Abstract

Characteristics of wavepacket and wedge shaped disturbances propagating in a boundary layer on the wing of the experimental airplane of *Next Generation Supersonic Transport (NEXST-1)* was numerically investigated using a saddle-point method and a complex ray theory. The NEXST-1 project has been conducted by *National Aerospace Laboratory of Japan (NAL)*, and will be launched in year 2004. The wing model of the NEXST-1 was designed using the natural-laminar-flow (NLF) concept to reduce the friction drag. Since the estimation of the onset of transition from laminar to turbulent flow of the boundary layer on NEXST-1 wing model is an important subject in this project, the stability and transition analysis of the flow is made using the e^N method. To predict the transition location precisely, authors deal with more actual disturbances, wavepacket and wedge shaped disturbance, for the stability analysis. For describing the wavepacket disturbance, the saddle-point method developed by Cebeci, Stewartson and Chen is adopted and the complex ray theory developed Itoh for the wedge shaped disturbance. The velocity and temperature profiles were obtained by solving the compressible boundary layer equations with the infinite swept wing assumption. Numerical results obtained from the present study showed that the amplitude of disturbance are growing rapidly near the leading edge but the growth rate gets slow down soon thereafter. These properties are almost same between the saddle-point method and complex ray theory. It is seen that this wing model has wide laminar region

near the mid-span and the NLF concept was validated.

1 Introduction

NAL is conducting a research project in order to establish advanced technology for the NEXST, which is designed to cruise at Mach 2¹. A major task of this project is to validate the aerodynamic design based on computational fluid dynamics (CFD) by flight tests. In the first phase of the flight tests, a 1/8 scaled non-propulsive experimental airplane will be launched by rockets, and glide at altitudes of 15-18 km. Few hundred sensors mounted on the surface of the airplane will be used to detect the pressure distribution and other physical signals. Figure 1 shows a sketch of the experimental airplane.

The NEXST-1 wing was designed using the NLF concept to reduce the friction drag. The objective of the present study is to predict the transition location on the NEXST-1 wing using linear stability analysis.

2 Velocity Profiles and Stability Analysis

2.1 Velocity Profiles

The compressible boundary layer equations need to be solved first to obtain the velocity and temperature profiles for stability analysis. With the infinite swept wing assumption, variations of flow in span-wise direction are neglected and the span-wise momentum equation is decoupled from the stream-wise momentum equation. The

inviscid velocity and pressure distributions on the surface of the wing was provided by the NEXST project center at NAL of Japan and used as external boundary conditions. The boundary layer equations were solved using the Keller's box method²

2.2 C-S-C Saddle-Point Method

In order to determine the onset of transition from laminar to turbulent flow of NEXST-1 wing model, the saddle-point method of Cebeci, Stewartson and Chen^{3,4,5} was used to solve the linearized compressible stability equations. The linearized compressible stability equations and their boundary conditions are given in Reference 6 and were solved by the Keller's box scheme. Since the linearized compressible stability equations and their boundary conditions are both homogeneous, the solutions of them reduce to an eigenvalue problem involving unknowns of wave numbers (α and β) and frequencies. The eigenvalue problem can be formulated based on the concept of group velocity^{3,4,5} such that the relationship between the two wave numbers are determined from the requirement that $\frac{\partial \alpha}{\partial \beta}$ is real. According to the group velocity concept, the direction of wave propagation is given by

$$\left(\frac{\partial \alpha}{\partial \beta} \right)_{\omega, R} = -\tan \gamma = -\frac{z}{x} \quad (1)$$

where γ denotes the angle that the direction of wave propagation makes with the x-axis.

In the saddle-point method, stability calculation is started by determining the wave numbers and frequencies of the disturbances at a specified x/c location using zarfs^{3,4,5} which correspond to the envelope of neutral stability curves for three-dimensional flows. Once the frequency is determined from zarfs, the amplification rate of the disturbance with a specified frequency is given by

$$\Gamma = \beta_i \left(\frac{\partial \alpha}{\partial \beta} \right)_{\omega, R} - \alpha_i \quad (3)$$

For a specified dimensional frequency, the eigenvalue procedure is used to calculate the wave numbers at downstream locations. Values of $\frac{\partial \alpha}{\partial \beta}$ will be varied in order to maximize the

amplification rate. The onset of transition can be determined using the e^N method^{7,8} by evaluating the amplification factor

$$N = \int_{x_0}^x \Gamma dx \quad (4)$$

for a set of specified dimensional frequencies in order to find the critical frequency that is most amplified. The stability analysis will be executed at different span-wise stations of the wing to determine the onset of transition from laminar to turbulent flow. Predictions from stability analysis will be used to validate the NLF concept quantitatively.

2.3 Complex Ray Theory

The complex ray theory was developed by Itoh⁹ on the basis of the kinematic wave theory. In this theory, disturbance wave is represented by the plane wave form with complex phase function Θ , and the complex wavenumber and frequency are then determined in the form

$$\frac{\partial \Theta}{\partial Y} = \frac{\beta}{\Delta}, \quad \frac{\partial \Theta}{\partial X} = \frac{\alpha}{\Delta}, \quad \frac{\partial \Theta}{\partial T} = -\frac{\omega}{\Delta^*}, \quad (5)$$

where Δ and Δ^* are scale function. From these relation, we can obtain the compatibility conditions

$$\begin{aligned}\frac{\partial}{\partial Y}\left(\frac{\alpha}{\Delta}\right) &= \frac{\partial}{\partial X}\left(\frac{\beta}{\Delta}\right), \\ \frac{\partial}{\partial T}\left(\frac{\alpha}{\Delta}\right) &= -\frac{\partial}{\partial X}\left(\frac{\omega}{\Delta^*}\right), \\ \frac{\partial}{\partial T}\left(\frac{\beta}{\Delta}\right) &= -\frac{\partial}{\partial Y}\left(\frac{\omega}{\Delta^*}\right).\end{aligned}\quad (6)$$

For the wedge shaped disturbance, imaginary part of ω and the differentiation with respect to T may be equated to 0. Then the compatibility conditions (5) can be simplified to the form

$$\frac{\partial}{\partial X}\left(\frac{\beta}{\Delta}\right) + \frac{\omega_\beta}{\omega_\alpha} \frac{\partial}{\partial Y}\left(\frac{\beta}{\Delta}\right) = 0. \quad (7)$$

This equation implies that β/Δ is constant on the ray defined by

$$\frac{dY}{dX} = \frac{\omega_\beta}{\omega_\alpha}. \quad (8)$$

When the dispersion relation and the complex group velocity $\omega_\alpha/\omega_\beta$ are rewritten in the form

$$\hat{\alpha} \equiv \frac{\alpha}{E_1\Delta} = \alpha(X; \hat{\beta}, \hat{\omega}), \quad C \equiv \frac{\omega_\beta}{\omega_\alpha} = C(X; \hat{\beta}, \hat{\omega}), \quad (9)$$

then we can obtain the following equations.

$$Y_r = \int_{X_0}^{X_1} C_r(X; \hat{\beta}, \hat{\omega}) dX, \quad (10)$$

$$Y_i = \int_{X_0}^{X_1} C_i(X; \hat{\beta}, \hat{\omega}) dX = 0, \quad (11)$$

and N factor

$$N = E_2 \int_{X_0}^{X_1} [\hat{\alpha}_i(X; \hat{\beta}, \hat{\omega}) + C_r(X; \hat{\beta}, \hat{\omega})] dX, \quad (12)$$

where E_1 and E_2 are constant and $\hat{\beta}$, $\hat{\omega}$ are defined by

$$\hat{\beta} \equiv \frac{\beta}{E_1\Delta} = \beta(X; \hat{\beta}, \hat{\omega}), \quad \hat{\omega} \equiv \frac{\omega}{E_1\Delta^*} = \omega(X; \hat{\beta}, \hat{\omega}), \quad (13)$$

and X_0 , X_1 denote the source and observation point of disturbance.

3 Numerical Results

3.1 C-S-C Saddle-Point Method

The NEXST-1 experimental airplane is about 11.5m long and the semi span length S is 2.36m. The stability analyses were done on eight span-wise sections normal to the leading edge of the wing under the condition of flight test Mach 2. The leading edge points of these sections are located at $Y/S = 0.2, 0.3, 0.4, 0.5, 0.6, 0.7, 0.8, 0.9$, respectively. Figure 2 shows the pressure distribution and the external velocity components in the direction normal and parallel to the leading edge at $Y/S=0.3$. The horizontal axis gives the surface distance from the leading edge. The most remarkable feature of this figure is the rapid variation of the pressure, which tends to minimize the cross-flow velocity components and is efficient in suppressing the cross-flow instability.

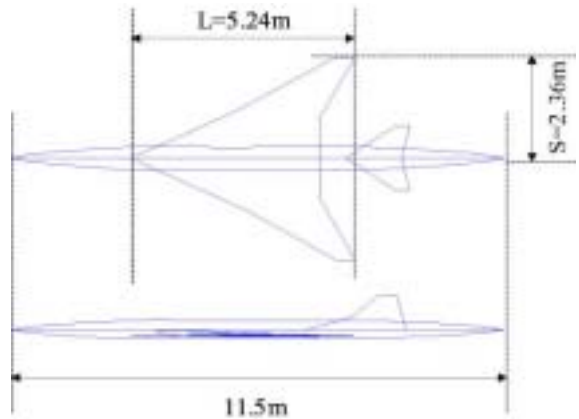


Fig 1. The NEXST-1 experimental airplane.

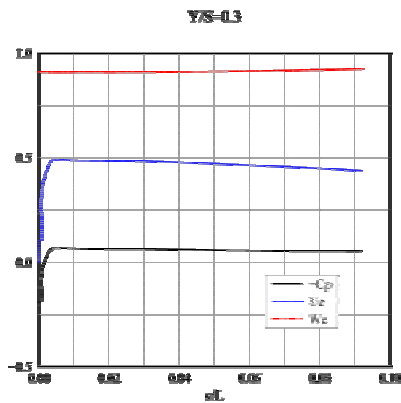


Fig. 2. The pressure and external velocity at Y/S=0.3

Fig. 3 shows the zarf near the leading edge at Y/S=0.3. The N factors for several frequencies corresponding to points indicated in Fig. 3 are shown in Fig. 4. From this figure, it is found that the disturbance waves grow rapidly near the leading edge and then grow mildly. This indicates that the cross flow instability is dominant near the leading edge. Table 1 shows critical frequencies and the corresponding maximum values of N factor at each wing section. Contour of the N factors corresponding to N = 8, 10, 12, and 14 is shown in Fig. 6. It is seen that although the N factor becomes larger near the wing root and wing tip, the NLF concept is validated around the mid-span as shown by the smaller value of N factors in this region.

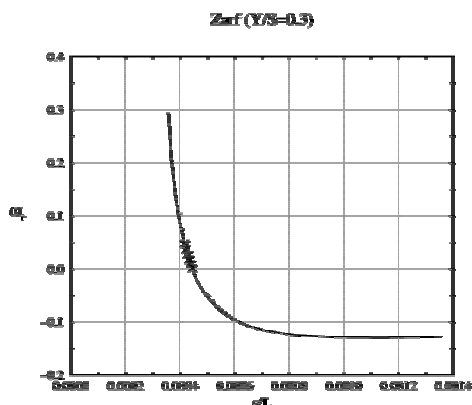


Fig. 3 Zarf near the leading edge at Y/S=0.3

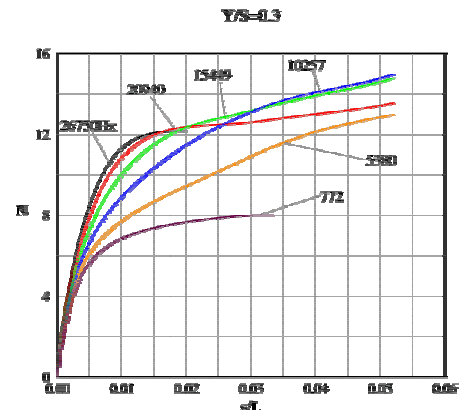


Fig. 4 N factor for several frequencies at Y/S=0.3.

3.2 Complex Ray Theory

In this section, the analysis is done for only one disturbance with the frequency $f=10\text{kHz}$ at location $X/S=0.3$ at same Mach number of previous analysis but under wind tunnel test condition. Since the frequency of disturbance is fixed, the remaining parameter is only $\hat{\beta}$ in this theory. Then $\hat{\beta}$ is restricted to real value in order to simplify. For each value of $\hat{\beta}_r$, the location X satisfying the equation (11) is obtained as different value. Figure 7 shows the variation of Y and N factor for three different value of $\hat{\beta}_r$, namely $\hat{\beta}_r=480, 550,$ and 1500 . In the case of $\hat{\beta}_r=480$ for example, Y_i equated to 0 at about $X=0.325$. So observation point of this disturbance is about $(X,Y)=(0.325,0.7)$, and the N factor at this point is about 7. With same procedure is made for various value of $\hat{\beta}_r$, a continuous line of N factor on the chord line can be obtain as in Fig.8. Furthermore observation location of the most amplified disturbance with each value of $\hat{\beta}_r$ is given in Fig.9. It is find from this figure that the propagation location of most amplified disturbances swerve from the chord line as convection.

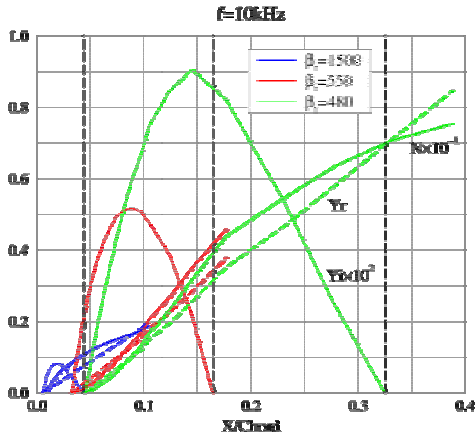


Fig.7 Variation of Y and N factor.

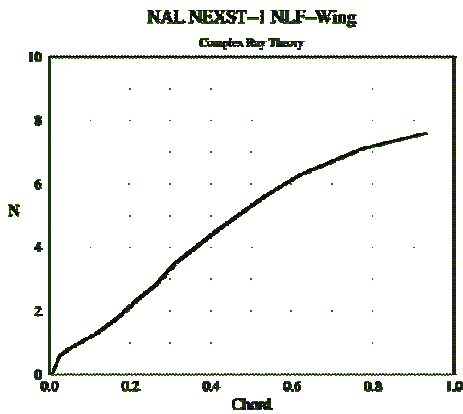


Fig.8 Variation of N factor on the Chord line.

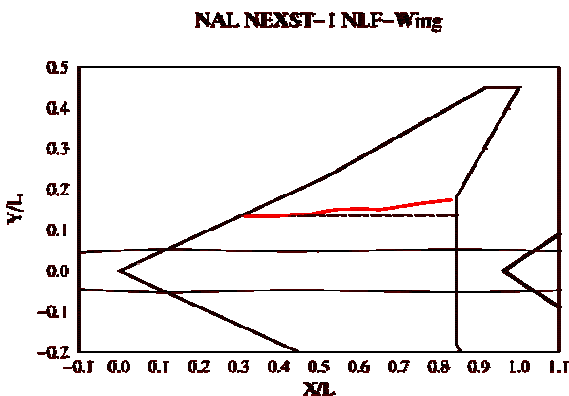


Fig.9. Propagation location of the most amplified disturbances introduced at leading edge of $Y/S=0.3$.

4 Conclusion

Stability and transition analysis of NEXST-1 wing model at Mach 2 was carried out using the e^N method with the saddle-point method of Cebeci, Stewartson and Chen, and a complex ray theory of Itoh. For the saddle-point analysis, the concept of zarf is also used to determine the critical frequency and the point to start the stability analysis. The calculations were then executed at eight span-wise sections of the wing. It is seen from the results that although cross-flow instability is dominant near the leading edge, the N factor does not grow too much except for regions near the wing root and wing tip. From the analysis of the complex ray theory, variation of the N factor on the chord line and the property of propagation of most amplified disturbance are clearly shown. From these results, there is no discrepancy between two analyses with different description of disturbance wave, and it can be concluded that the NLF concept was validated. The present study will be extended to full three-dimensional analysis without making the infinite swept wing assumption in the near future.

Acknowledgement

We would like to express our gratitude to Dr.K.Yoshida, Dr.K.Ueda, and Dr.H.Ishikawa at NAL of Japan for providing helpful advices and aerodynamic data for the NEXST-1 wing model.

References

- [1] Yoshida,K., Makino, Y., and Shimbo, Y. "An Experimental Study on Unmanned Scaled Supersonic Experimental Airplane," AIAA Paper 2002-2842, June, 2002.
- [2] Cebeci, T., "An Engineering approach to the Calculation of Aerodynamic Flows," Springer Verlag, Dec. 1999.
- [3] Cebeci, T. and Stewartson, K., "Stability and Transition in Three-Dimensional Flow," AIAA J., Vol. 28, pp.398-405, 1980.

- [4] Cebeci, T., and Chen, H.H., "Numerical Method for Predicting Transition in Three-Dimensional Flows by Spatial Amplification Theory," AIAA J., Vol. 30, No.8, pp.1972-1979, 1992.
- [5] Cebeci, T., Chen, H. H. and Arnal, D., "Natural Transition in Compressible Flows on Wings: Spatial Theory and Experiment," AIAA Paper 94-0824, Jan. 1994.
- [6] Malik, M. R., "COSAL – A Black Box Compressible Stability Analysis Code for Transition Prediction in Three-Dimensional Boundary Layers," NASA CR 165-925, 1982.
- [7] Smith, A. M. O. and Gamberoni, N., "Transition, Pressure Gradient and Stability Theory," Douglas Aircraft Co. Rept. ES 26388, El Segundo, California, 1956.
- [8] Van Ingen, J. L., "A Suggested Semi-empirical Method for the Calculation of the Boundary Layer Transition Region," Univ. of Tech., Dept. of Aero. Eng. Rept.UTH-74, Delft, 1956.
- [9] Itoh, N., "Development of wedge-shaped disturbances originating from a point source in a three-dimensional boundary layer," Fluid Dyn. Res., vol. 18, pp.337-354, 1996.